Single-crystal Structure and Solid-state NMR of $Ga_{2-x}Sc_xO_3$ ($x = 0.83$)

Hamdi Ben Yahia[a], Leo van Wüllen[b], Sarkarainadar Balamurugan[a], Ute Ch. Rodewald[a], Hellmut Eckert[b], and Rainer Pöttgen[a]

[a] Institut für Anorganische und Analytische Chemie, Universität Münster, Corrensstraße 30, 48149 Münster, Germany
[b] Institut für Physikalische Chemie, Universität Münster, Corrensstraße 30, 48149 Münster, Germany

Reprint requests to R. Pöttgen. E-mail: pottgen@uni-muenster.de

Z. Naturforsch. **2011**, *66b,* 14 – 20; received October 29, 2010

Colorless needles of $Ga_{2-x}Sc_xO_3$ (x = 0.83) were isolated during the crystal growth of $La_3Ga_3Sc_2O_{12}$ in a K_2WO_4 flux. The structure was refined from X-ray single-crystal data: β-Ga_2O_3 type, $C2/m$, $Z = 4$, a = 12.716(4), b = 3.1566(6), c = 5.928(5) Å, β = 102.57(3)°, V = 232.2 Å^3, $wR2$ = 0.0618, 429 F^2 values, 32 variables. The structure is based on infinite double chains of edge-sharing Sc/GaO_6 octahedra running along the b axis. The GaO_4 tetrahedra connect these chains by sharing corners and form a three-dimensional framework. The oxygen atoms form a distorted *ccp* pattern. The ^{45}Sc NMR spectra confirm the presence of a single scandium site, while ^{71}Ga NMR data clearly prove the partial occupancy of the scandium site by gallium atoms. The nuclear electric quadrupolar parameters of ^{45}Sc and ^{71}Ga are discussed in relation to the crystallographic atomic environments.

Key words: Scandium, Crystal Chemistry, Solid-state NMR

Introduction

The sesquioxides Al_2O_3, Ga_2O_3, Sc_2O_3, and In_2O_3 find broad technical application. Al_2O_3 is a widely used abrasive and crucible material and an excellent material for electronic substrates. Tin-doped In_2O_3 (ITO) finds application in diverse transparent electrode materials of solar cells and opto-electronic devices. β-Ga_2O_3 (direct band gap of *ca.* 5 eV) has also been widely tested as a transparent electrode material. Sc_2O_3 produces high-index film layers that are transparent to wavelengths as short as 225 nm in the UV region. Such Sc_2O_3 films are insoluble and hard. Their high refractive index value makes them preferred materials for diverse optical coatings.

The four oxides have multiple cation sites, and solid solutions with two different trivalent cations are possible. Ordered structures have been reported for $ScAlO_3$ [1] and $ScInO_3$ [2, 3]. In the course of our systematic ^{45}Sc solid-state NMR spectroscopic investigations of intermetallic [4] and oxidic [5, 6] scandium compounds, we were interested in the solid solution $Ga_{2-x}Sc_xO_3$.

The phase equilibrium diagram of the quasibinary system Sc_2O_3–Ga_2O_3 was first determined by Schneider and Waring [7]. They reported the existence of two binary phases: (i) $6Sc_2O_3 \cdot 5Ga_2O_3$ with orthorhombic symmetry (a = 13.85, b = 9.80, c = 9.58 Å) and (ii) a phase called 'Uss' which is a solid solution that exists from 55 to 73 mole percent Ga_2O_3 at the solidus. Its compositional range of stability decreases to 61 mole percent Ga_2O_3 at 1440 °C. Later MacDonald *et al.* reinvestigated the 'Uss' phase and obtained a powder pattern identical to that reported by Schneider and Waring and concluded that the 'Uss' phase is ideally $GaScO_3$ [8]. These authors grew single crystals from a Bi_2O_3 flux and determined the orthorhombic symmetry with lattice parameters of a = 3.11, b = 18.92 and c = 7.33 Å. Based on a comparison of the powder patterns, MacDonald *et al.* noted some similarities with monoclinic β-Ga_2O_3 [9, 10], however, no complete structure determination was performed. Recently, Kuz'micheva *et al.* were able to grow single crystals of this phase by the Czochralski method starting from an equimolar mixture of Sc_2O_3 and Ga_2O_3 [11]. The authors noticed a variation of the composition $Ga_{2-x}Sc_xO_3$ ($0.42 \leq x \leq 0.52$) along the growth direction of the crystal as well as radially. Most of the diffraction peaks of the powder pattern obtained from crushed single crystals were indexed with a monoclinic β-Ga_2O_3-type cell [4]. Additional weak reflections were ascribed to superstructure formation due to

0932–0776 / 11 / 0100–0014 \$ 06.00

an ordering of Sc and Ga on the octahedral sites of the β-Ga_2O_3 structure. A preliminary structure refinement led to a structural model for $Ga_{1.5}Sc_{0.5}O_3$, however, with $R = 18\,\%$.

During crystal growth experiments with $La_3Ga_3Sc_2O_{12}$ in a K_2WO_4 flux at relatively low temperature (1200 °C) we obtained well-shaped transparent needles of $Ga_{2-x}Sc_xO_3$ ($x = 0.83$). Herein we report on an accurate crystal structure refinement and a solid-state NMR (^{45}Sc and ^{71}Ga) spectroscopic study of the $x = 0.83$ member of the solid solution $Ga_{2-x}Sc_xO_3$.

Experimental Section

Synthesis

The crystal used for the single-crystal investigation was grown from a K_2WO_4 flux, during the preparation of $La_3Ga_3Sc_2O_{12}$ single crystals. 100 mg of a pure $La_3Ga_3Sc_2O_{12}$ sample were thoroughly mixed in an agate mortar with 700 mg of K_2WO_4. The mixture was placed in a platinum crucible and fired at 1200 °C for 18 h and then cooled to 700 °C at a rate of 25 $°C\,h^{-1}$. Finally the sample was quenched to r. t. by pulling the crucible out of the furnace. The K_2WO_4 flux was dissolved in hot diluted HCl. This led to a mixture of three phases, (i) single crystals of $Ga_{2-x}Sc_xO_3$ with $x = 0.83$, (ii), $La_3Ga_3Sc_2O_{12}$ powder, and (iii) a non-identified phase (powder). The powders were removed by re-suspending the solid product in a large test tube using acetone. The test tube was sonicated in an ultrasonic cleaner for 1 min and then allowed to stand for 30 s. During that time the crystals of $Ga_{2-x}Sc_xO_3$ ($x = 0.83$) settled to the bottom of the test tube. The supernatant, containing the fine powder in suspension, was then decanted into another beaker. This process was repeated several times until the supernatant over the $Ga_{2-x}Sc_xO_3$ ($x = 0.83$) crystals was clear. Pure $Ga_{2-x}Sc_xO_3$ ($x = 0.83$) samples were then prepared by a ceramic route starting from a stoichiometric mixture of Ga_2O_3 and Sc_2O_3. Two pellets were made and heated at 1400 °C for 60 h. One was cooled slowly to r. t., and one was quenched in water from 1400 °C.

EDX data

Semiquantitative EDX analyses of many crystals including the one investigated on the diffractometer (Fig. 1) were carried out with a Leica 420i scanning electron microscope with GaP and Sc as standards. The experimentally observed compositions were close to the ideal one.

X-Ray diffraction

The polycrystalline samples were characterized by Guinier patterns (imaging plate detector, Fujifilm BAS-1800) with Cu$K_{\alpha 1}$ radiation and α-quartz ($a = 4.9130$, $c = 5.4046$ Å) as an internal standard. Using the cell parameters obtained by single-crystal diffraction, a full pattern matching refinement was performed with the JANA2006 program package [12]. The background was estimated by a Legendre function, and the peak shapes were described by a pseudo-Voigt function (Fig. 2). The refined lattice parameters for both samples (quenched and unquenched) were similar: $a = 12.717(2)$, $b = 3.1555(4)$, $c = 5.9307(7)$ Å, $\beta = 102.53(1)°$. No superstructure reflections have been observed.

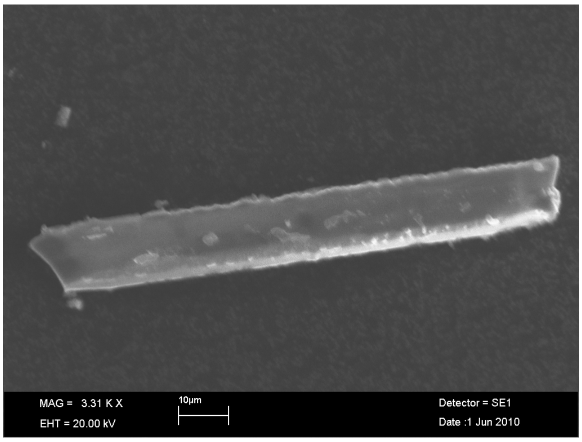

Fig. 1. Scanning electron micrograph of the $Ga_{2-x}Sc_xO_3$ ($x = 0.83$) single crystal used for the X-ray data collection.

A crystal suitable for single-crystal X-ray diffraction was selected on the basis of the size and the sharpness of the diffraction spots by Laue photographs on a Buerger camera (using white Mo radiation). The data collection was carried out at room temperature on a Stoe IPDS II diffractometer using MoK_α radiation. Data processing and all refinements were performed with the JANA2006 program package [12]. A Gaussian-type absorption correction was applied, and the shape was determined with the video microscope of the Stoe CCD camera. Details of the data collection and crystallographic parameters are summarized in Table 1.

Structure refinement

The extinction conditions observed for the $Ga_{2-x}Sc_xO_3$ ($x = 0.83$) crystal agree with the space groups $C2/m$, $C2$, and Cm. The structure was solved using the centrosymmetric space group $C2/m$ and the atomic positions of β-Ga_2O_3 [9]. The scandium and the gallium atoms were set in the octahedral and tetrahedral sites, respectively. The refinement of all the atomic positions and the isotropic displacement parameters led to the residual factors $R(F)/wR(F^2) = 0.0461/0.1027$ and a goodness of fit of $S = 1.72$ for 16 parameters and 432 reflections. With anisotropic displace-

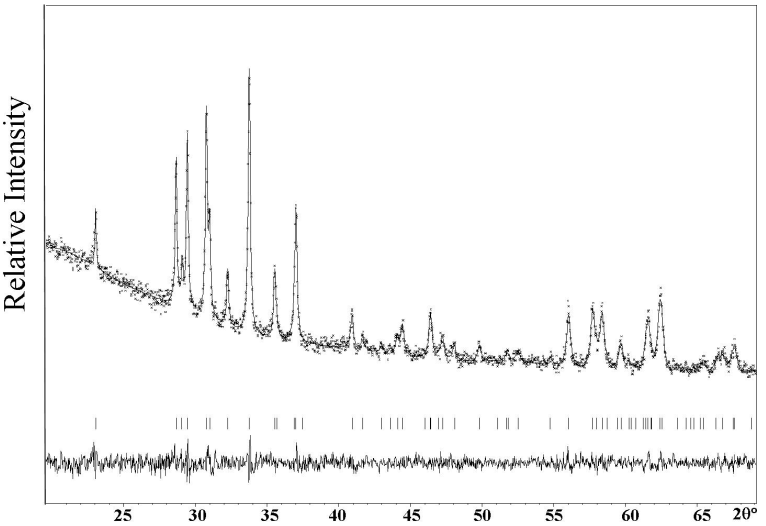

Fig. 2. Observed, calculated and difference plots for the XRPD profile refinement of the $Ga_{2-x}Sc_xO_3$ ($x = 0.83$) sample.

Table 1. Crystallographic and structure refinement data for $Ga_{2-x}Sc_xO_3$ ($x = 0.83$).

Formula	$Ga_{1.17}Sc_{0.83}O_3$
Crystal	colorless needle
M_r	166.7
Crystal system	monoclinic
Space group	$C2/m$
Lattice parameters	
a, Å	12.716(4)
b, Å	3.1566(6)
c, Å	5.928(5)
β, deg	102.57(3)
Cell volume V, Å^3	232.2
Z	4
Density calc., g cm^{-3}	4.77
$F(000)$, e	311
Scan mode	multi-scan
hkl range	±20, ±5, ±9
θ_{min} / θ_{max}, deg	3.28 / 34.88
Linear absorption coeff., mm^{-1}	14.2
Absorption correction	GAUSSIAN
T_{min} / T_{max}	0.474 / 0.838
No. of reflections	1778
No. of independent reflections	580
R_{int}	0.0606
Reflections used [$I \geq 2\sigma(I)$]	429
No. of refined parameters	32
R factors $R(F)$ / $wR(F^2)$	0.0326 / 0.0618
S (GoF)	1.05
Weighting scheme	$w = 1/(\sigma^2(I) + 0.0009I^2)$
Diff. Fourier resid. min / max, e Å^{-3}	−0.92 / +1.21

ment parameters for all positions, the residual factors converged to $R(F)/wR(F^2) = 0.0391$ / 0.0839 and $S = 1.43$ for 32 refined parameters. This led to the ideal composition $GaScO_3$. Refinement of the Ga and Sc occupancies showed a significant deviation from the ideal value for the scandium site. Subsequently we refined this site with a mixed Sc/Ga occupancy. This significantly decreased the reliability factors $R(F)/wR(F^2) = 0.0326$ / 0.0618 and $S = 1.05$, leading to the composition $Ga_{1.17(2)}Sc_{0.83(2)}O_3$ for the investigated crystal. The refined atomic positions and anisotropic displacement parameters (ADPs) are given in Tables 2 and 3.

Table 2. Atom positions and equivalent isotopic displacement parameters (Å^2) for $Ga_{2-x}Sc_xO_3$ ($x = 0.83$). All atoms lie on Wyckoff sites 4*i*. The mixed-occupied site has 83 % Sc + 17 % Ga.

Atom	x	y	z	U_{eq}
Sc1 / Ga1	0.34476(6)	0	0.68860(12)	0.0073(2)
Ga2	0.09042(5)	0	0.79171(9)	0.00623(15)
O1	0.1588(3)	0	0.0963(6)	0.0093(9)
O2	0.4889(3)	0	0.2552(5)	0.0071(8)
O3	0.8273(3)	0	0.4315(5)	0.0068(8)

Table 3. Anisotropic displacement parameters (Å^2) for $Ga_{2-x}Sc_xO_3$ ($x = 0.83$). The anisotropic displacement factor exponent takes the form: $-2\pi^2[(ha^*)^2U_{11} + \ldots + 2hka^*b^*U_{12}]$. $U_{12} = U_{23} = 0$.

Atoms	U_{11}	U_{22}	U_{33}	U_{13}
Sc1 / Ga1	0.0085(3)	0.0063(4)	0.0073(3)	0.0021(2)
Ga2	0.0086(3)	0.0056(3)	0.0050(2)	0.00261(15)
O1	0.0120(15)	0.0100(18)	0.0051(12)	0.0002(11)
O2	0.0076(14)	0.0059(16)	0.0077(12)	0.0018(10)
O3	0.0083(13)	0.0077(16)	0.0058(12)	0.0042(9)

Further details of the crystal structure investigation may be obtained from Fachinformationszentrum Karlsruhe, 76344 Eggenstein-Leopoldshafen, Germany (fax: +49-7247-808-666; e-mail: crysdata@fiz-karlsruhe.de, http://www.fiz-informationsdienste.de/en/DB/icsd/depot_anforderung.html) on quoting the deposition number CSD-422271.

Solid-state NMR spectroscopy

^{45}Sc magic-angle spinning (MAS) NMR spectra were recorded at ambient temperature at resonance frequencies of 97.176 MHz on a Bruker DSX-400 spectrometer, using a 2.5 mm MAS NMR probe operated at a rotation frequency of 20 – 25 kHz. Spectra were recorded using a single pulse acquisition with a 0.5 μs pulse length and a recycle delay of 2 s. The ^{45}Sc NMR resonance shifts are referenced to 0.1 M scandium chloride aqueous solution. Simulated lineshapes were obtained using the DMFIT program [13]. ^{71}Ga NMR spectra were obtained on a Bruker Avance III 300 spectrometer at 91.57 MHz. Spin echo trains generated *via* a Q-CPMG pulse sequence [14], $\theta - \tau_1 - 2\theta - [\tau_2 - 2\theta - \tau_2]_n$ ($n = 160$), were acquired at a ^{71}Ga nutation frequency of 71 kHz, using a flip angle θ of 38.5°. 1000 echo trains were co-added, using a recycle delay of 10 s. Subsequent Fourier transformation of these echo trains yielded a "spikelet pattern", the overall envelope of which corresponded to the static NMR lineshape. In the present case, the overall spectral intensity is distributed over an extremely wide spectral region. The position of the carrier was systematically varied from +2000 to −2000 ppm in thirteen 30-kHz steps. The total lineshape was then synthesized by superimposing all of the spikelet spectra obtained at the different carrier frequencies and simulated using the DMFIT software. Resonance shifts are given relative to a 1 M $Ga(NO_3)_3$ solution. Theoretical electric field gradient calculations were conducted using the WIEN2k package [15] employing the prodecure and parameters described in [16]. The R(MT) parameters were 1.99, 1.68 and 1.68 a. u. for Sc, Ga and O, respectively, and a separation energy of −8.0 Ry was used.

Results

The structure of $Ga_{2-x}Sc_xO_3$ ($x = 0.83$) is isotypic with β-Ga_2O_3 [9, 10]. The monoclinic β-Ga_2O_3 structure contains two crystallographically non-equivalent gallium and three oxygen sites, all of them located at 4*i* (*x*, 0, *z*) positions. The structure is based on infinite double chains of edge sharing Sc1/Ga1O_6 octahedra running along the *b* axis. The Ga2O_4 tetrahedra connect these chains by sharing corners and form a three-dimensional framework (Fig. 3). The oxygen atoms show a distorted *ccp* pattern. The partition of Sc^{3+} and Ga^{3+} onto octahedral and tetrahedral sites is in line with the difference in the ionic radii [17] of 0.61 Å (Ga^{3+} for coordination number 4) and 0.885 Å (Sc^{3+} for coordination number 6). The Sc1/Ga1 mixing can be rationalized, since the ionic radii of Ga^{3+} and Sc^{3+} for coordination number 6 are similar.

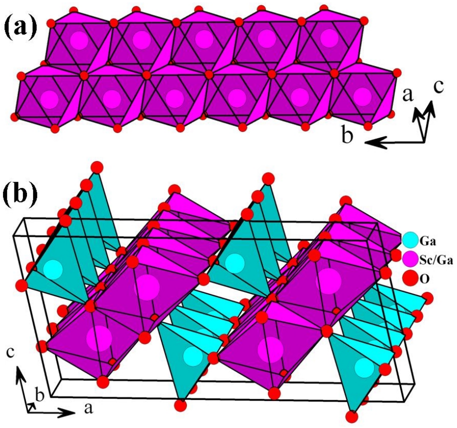

Fig. 3 (color online). (a) View of the double chains of ScO_6 octahedra sharing edges and (b) perspective view of the structure of $Ga_{2-x}Sc_xO_3$ ($x = 0.83$).

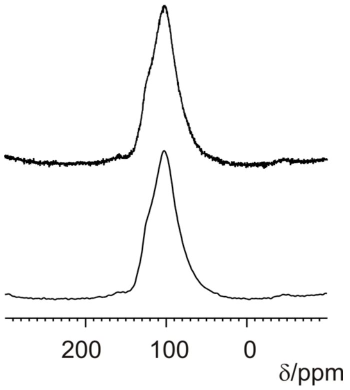

Fig. 4. ^{45}Sc MAS NMR spectra of the unquenched (top) and quenched (bottom) sample of $Ga_{2-x}Sc_xO_3$ ($x = 0.83$). Spinning speed: 20 kHz.

Fig. 4 shows the ^{45}Sc magic-angle spinning MAS NMR spectra obtained for a quenched and an annealed sample. Identical spectra are observed, characterized by an isotropic chemical shift of 131.5 ppm, a quadrupolar coupling constant (C_Q) of 9.6 MHz and an electric field gradient asymmetry parameter (η_Q) of 0.7. These results are in reasonable agreement with calculated values of C_Q (theor.) = 8.4 MHz and $\eta = 0.92$ using the programme WIEN2k. Fig. 5 shows the static ^{71}Ga spikelet NMR spectrum of this compound. The envelope can be simulated successfully as a superposition of two static spectra, in an approximate ratio of 86 : 14 (see Fig. 5), which is in excellent agreement with the information from the crystal structure. Table 5 summarizes the values of the nuclear electric quadrupolar coupling con-

Table 4. Interatomic distances (Å) and bond valence sums (BVS, with coordination numbers in brackets) for $Ga_{2-x}Sc_xO_3$ ($x = 0.83$). Average distance and angle values are given in brackets. For the mixed-occupied site the BVS values have been calculated separately for Sc (larger values) and gallium (smaller values).

	Distance	B.V.		Distance	B.V.
Sc1/Ga1–O1 (2×)	2.036(3)	0.603/0.437	Ga2–O1	1.826(4)	0.771
Sc1/Ga1–O2	2.069(4)	0.552/0.400	Ga2–O2 (2×)	1.8608(18)	0.702
Sc1/Ga1–O3 (2×)	2.172(3)	0.418/0.303	Ga2–O3	1.857(4)	0.709
Sc1/Ga1–O3	2.149(4)	0.444/0.322		⟨1.851⟩	BVS [4] = 2.884
	⟨2.105⟩	BVS [6] = 3.038/2.202			

BV = $e^{(r0-r)/b}$ with the following parameters: $b = 0.37$, r_0 (Ga^{III}–O) = 1.730 and r_0 (Sc^{III}–O) = 1.849 [19, 20].

Table 5. Experimental isotropic chemical shifts and nuclear electric quadrupolar coupling parameters and comparison with predicted values (in parentheses) using the program WIEN2k.

Site	$\delta_{cs}{}^{iso}$ (ppm)	C_Q (MHz) (±0.5 MHz)	η (±0.1)
Ga(1)	-15 ± 10	5.6 (4.1)	0.5 (0.9)
Ga(2)	222 ± 50	14.4 (13.0)	0.5 (0.62)

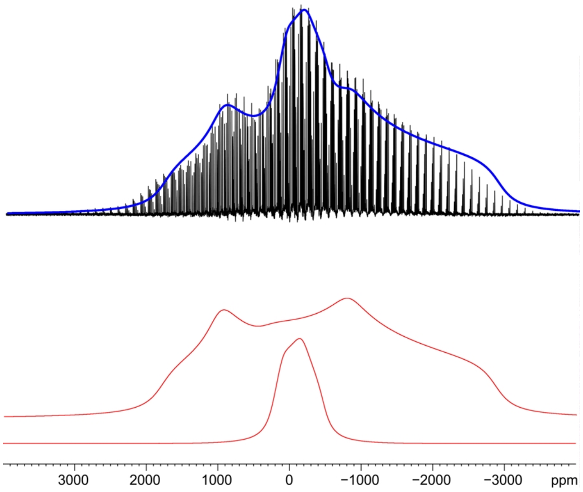

Fig. 5 (color online). Experimental and simulated ^{71}Ga NMR spectrum of $Ga_{2-x}Sc_xO_3$ ($x = 0.17$). Top: Superimposed experimental spikelet spectra, together with a simulation of the intensity profile envelope. Bottom: Simulated individual lineshape components.

stant C_Q, the electric field gradient asymmetry parameter η and isotropic chemical shift values δ_{CS} as they were extracted from the simulation yielding closest agreement with the experimental data. For the tetrahedral Ga(2) site, the experimentally measured electric field gradient parameters are in good agreement with theoretically calculated values. Furthermore, the chemical shift deduced for this site falls into the general shift range published for tetrahedral gallium sites [18]. For the octahedrally coordinated Ga(1) site, the chemical shift also falls into the range of shifts previously published for octahedrally coordinated gallium species in crystalline inorganic oxides [18].

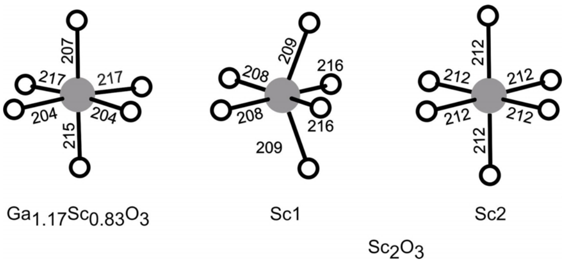

Fig. 6. Oxygen coordination of the scandium atoms in $Ga_{1.17}Sc_{0.83}O_3$ and Sc_2O_3. For details see text.

Discussion

The ^{45}Sc NMR results are in good agreement with the single-crystal X-ray diffraction data, which show that the scandium ions are solely located on octahedral sites. The octahedra are slightly distorted with three short and three normal Sc1–O distances or three normal and three stretched Ga1–O distances (Table 4). The average Sc1/Ga1–O distance of 2.105 Å is slightly shorter than 2.145 Å and longer than 2.02 Å, the sum of the ionic radii of Sc^{3+} and O^{2-}, and of Ga^{3+} and O^{2-}, respectively [17]. The calculated BVS value of 3.04 is in very good agreement with the expected 3+ value for Sc [19, 20], however, Ga1 on this site is underbonded with a BVS value of only 2.20. Indeed, the octahedral site is predominantly occupied with scandium, which is slightly bigger than gallium (*vide supra*). The Sc–O distances are similar to those in Sc_2O_3 (2.08 – 2.16 Å) [21, 22].

The scandium-oxygen polyhedra of $Ga_{1.17}Sc_{0.83}O_3$ and Sc_2O_3 are compared in Fig. 6. The Sc2 atoms in Sc_2O_3 show six equal Sc2–O distances of 212 pm, however, these octahedra are slightly compressed with O–Sc2–O angles of 80 and 100°. A much stronger distortion is evident for the Sc1 atoms with a broader range of Sc1–O distances from 208 to 216 pm and also

Table 6. Crystallographic data for $Ga_{2-x}Sc_xO_3$ (x = 0, 0.42, 0.52 and 0.83), space group $C2/m$, Z = 4.

Formula	β-Ga_2O_3	$Ga_{1.58}Sc_{0.42}O_3$	$Ga_{1.48}Sc_{0.52}O_3$	$Ga_{1.17}Sc_{0.83}O_3$
Growth method	PbO-Li_2O-B_2O_3 flux	Czochralski	Czochralski	K_2WO_4 flux
Refinement	method	single crystal	Rietveld	Rietveld single crystal
M_r	187.44	177.04	174.56	166.7
a, Å	12.214(3)	12.478(4)	12.496(4)	12.716(4)
b, Å	3.0371(9)	3.1010(4)	3.1013(4)	3.1566(6)
c, Å	5.7981(9)	5.8720(5)	5.8733(6)	5.928(5)
β, deg	103.83(2)	103.20(2)	103.26(1)	102.57(3)
Cell volume, Å^3	208.9	221.2	221.5	232.2
Density, g cm^{-3}	5.96	5.32	5.23	4.77
Reference	[10]	[11]	[11]	this work

a broader range of O–Sc1–O angles from 80 to 115°. As previously discussed [23], the different degrees of distortion give rise to significantly different ^{45}Sc EFG parameters. Consistent with the wider range of Sc–O distances and O–Sc–O bond angles, the C_Q value is significantly larger for the Sc1 site compared to the Sc2 site (23.4 *vs.* 15.3 MHz, respectively). Furthermore, the Sc1 site lies on a C_3 axis yielding an axially symmetric electric field gradient tensor, whereas for the Sc2 site the asymmetry parameter is non-zero. For $Ga_{1.17}Sc_{0.83}O_3$, the range of Sc–O bond lengths is comparable to that of Sc1 in Sc_2O_3, whereas the range of O–Sc–O angles (80 – 102°) is comparable to that for Sc2 in Sc_2O_3. The calculated and experimental C_Q values are, however, significantly smaller than for either of the two sites in scandium oxide. This comparison illustrates the difficulty in correlating quadrupolar coupling parameters with individual geometric distortion parameters in ^{45}Sc NMR.

The tetrahedral site is fully occupied by Ga2 and is highly distorted with angles ranging from 105.34 to 118.94° with an average O–Ga2–O value of 109.5°. The average Ga2–O distance of 1.851 Å is in good agreement with the expected value of 1.85 Å [17]. These values are very similar to those reported for β-Ga_2O_3 ($\langle$Ga–O$\rangle$ = 1.844 Å and $\langle$O–Ga–O$\rangle$ = 109.42°) [9]. The calculated BVS value of 2.884 shows that Ga2 is only slightly under-bonded. The strongly distorted gallium environments manifest themselves in an unusually large quadrupole coupling constant, which is comparable to that measured in β-Ga_2O_3 [18]. In contrast, the octahedral gallium species situated on the Sc1 sites have more symmetrical local environments, which facilitate their detection by ^{71}Ga NMR despite their low concentration. To compare the experimental quadrupolar coupling parameters for the six-coordinated gallium site in $Ga_{1.17}Sc_{0.83}O_3$ with a theoretical prediction, C_Q values were calculated by scaling the WIEN2k value obtained for ^{45}Sc with the ratio of the nuclear electric quadrupole moments of ^{71}Ga and ^{45}Sc. The agreement between experimental and calculated data is only moderate in this case, indicating that the Sc1 site, when occupied by Ga^{3+}, is locally distorted to a significant extent. This finding can be rationalized by the small difference in the ionic radii between Sc^{3+} and Ga^{3+}.

In order to compare our results with previous work, Table 6 summarizes all the important data related to the different compositions studied in the $ScGaO_3$-β-Ga_2O_3 system. One can conclude that the chemical composition of our crystal is in very good agreement with the evolution of the cell parameters. Indeed, since scandium is slightly bigger than gallium, the substitution of gallium for scandium induces an increase of the cell parameters. From the evolution of the cell parameters one might estimate those of $ScGaO_3$, the theoretical end member of this $ScGaO_3$-β-Ga_2O_3 system ($C2/m$, a = 12.808, b = 3.178, c = 5.954 Å, β = 102.39°, V = 236 Å^3). Experimentally, Schneider and Waring reported $Ga_{1.1}Sc_{0.9}O_3$ as the end member [7]. These results are very similar to those of $Ga_{1.2}In_{0.8}O_3$ [24], indicating that a total substitution of gallium for scandium or indium in the octahedral site of the β-Ga_2O_3 type induces a destabilization of the structure. Indeed, there is no $AGaO_3$ compound crystallizing with the monoclinic β-Ga_2O_3 type. Most $AGaO_3$ compounds crystallize with perovskite-related structures.

Acknowledgements

This work was financially supported by the Deutsche Forschungsgemeinschaft. H. B. Y. and S. B. are indebted to the Alexander von Humboldt Foundation for research stipends.

[1] W. Sinclair, R. A. Eggleton, A. E. Ringwood, *Z. Kristallogr.* **1979**, *149*, 307.
[2] R.-D. Shannon, *Solid State Commun.* **1966**, *4*, 629.
[3] B. I. Pokrovskii, L. N. Komissarova, L. M. Vasilleva, V. I. Chechernikov, A. V. Pechennikov, *Inorg. Mater.* **1966**, *2*, 1306.
[4] H. Eckert, R. Pöttgen, *Z. Anorg. Allg. Chem.* **2010**, *636*, 2232.
[5] S. Balamurugan, U. Ch. Rodewald, T. Harmening, L. van Wüllen, D. Mohr, H. Eckert, R. Pöttgen, *Z. Naturforsch.* **2010**, *65b*, 13.
[6] S. Balamurugan, U. Ch. Rodewald, T. Harmening, L. van Wüllen, D. Mohr, H. Deters, H. Eckert, R. Pöttgen, *Z. Naturforsch.* **2010**, *65b*, 1199.
[7] S. J. Schneider, J. L. Waring, *J. Res. Nat. Bur. Stand.* **1963**, *67A*, 19.
[8] J. MacDonald, J. A. Gard, F. P. Glasser, *J. Inorg. Nucl. Chem.* **1967**, *29*, 661.
[9] S. Geller, *J. Chem. Phys.* **1960**, *33*, 676.
[10] J. Åhman, G. Svensson, J. Albertsson, *Acta Crystallogr.* **1996**, *C52*, 1336.
[11] G. M. Kuz'micheva, V. B. Rybakov, S. A. Kutovoi, *Inorg. Mater.* **2004**, *40*, 1066.
[12] V. Petříček, M. Dušek, L. Palatinus, JANA2006, The Crystallographic Computing System, Institute of Physics, University of Prague, Prague (Czech Republic) **2006**.
[13] D. Massiot, F. Fayon, M. Capron, I. King, S. Le Calve, B. Alonso, J. O. Durand, B. Bujoli, Z. Gan, G. Hoatson, *Magn. Reson. Chem.* **2002**, *40*, 70.
[14] I. Hung, A. J. Rossini, R. W. Schurko, *J. Phys. Chem. A* **2004**, *108*, 7112.
[15] P. Blaha, K. Schwarz, G. K. H. Madsen, D. Kvasnicka, J. Luitz, WIEN2k, An Augmented Plane Wave Plus Local Orbitals Program for Calculating Crystal Properties, Vienna University of Technology, Vienna (Austria) **2001**.
[16] C. P. Sebastian, L. Zhang, C. Fehse, R.-D. Hoffmann, R. Pöttgen, *Inorg. Chem.* **2007**, *46*, 771.
[17] R. D. Shannon, *Acta Crystallogr.* **1976**, *A32*, 751.
[18] J. T. Ash, P. J. Grandinetti, *Magn. Reson Chem.* **2006**, *44*, 823.
[19] I. D. Brown, D. Altermatt, *Acta Crystallogr.* **1985**, *B41*, 244.
[20] N. E. Brese, M. O'Keeffe, *Acta Crystallogr.* **1991**, *B47*, 192.
[21] W. H. Zachariasen, *Skr. Nor. Vidensk.-Akad.* **1928**, 4.
[22] S. Geller, P. Romo, J. P. Remeika, *Z. Kristallogr.* **1967**, *124*, 136.
[23] N. Kim, C. H. Hsieh, J. F. Stebbins, *Chem. Mater.* **2006**, *18*, 3855,
[24] C. Vigreux, L. Binet, D. Gourier, B. Piriou, *J. Solid State Chem.* **2001**, *157*, 94.